Classical Laminate Theory
for laminates composed of unidirectional layers

J. Broede, T. Haberle

16.04.2024

Summary

The present document describes the analysis of laminates on the basis of the 2D continuum theory, assuming a plane stress state. The theory is referred to as the Classical Laminate Theory (CLT). It includes the Kirchhoff-Love plate theory and is used to determine the in-plane stresses and strains in each individual layer of the laminate.

Keywords: Classical laminate theory, laminate, layer, ply, elasticity relationships

References

[1] Jones, R. M.: Mechanics of Composite Materials. McGraw-Hill, 1975

[2] Ashton, J. E. and Whitney, J. M.: Theory of laminated plates. Technomic publishing Co, 1970

[3] J.N. Reddy: Mechanics of laminated composite plates and shells. Second edition. CRC Press, 2004

[4] VDI 2014: Development of Fibre-Reinforced Plastic Components; Sheet 3. Analysis. Beuth-Verlag, Berlin, 2006

1 General

The Classical Laminate Theory describes laminates composed of several layers. In the literature, the laminate is often referred to as multilayer composite (or short: composite), the layers are often named laminae or plies.

A laminate responds as a whole with a common continuous displacement field and a common continuous strain field. Only the stress field may have discontinuities for the membrane and bending stresses at the layer boundary surfaces.

The Classical Laminate Theory is a 2D theory. It is based on the assumptions of a plane stress state ($\sigma_z = \tau_{yz} = \tau_{zx} = 0$) and of the Kirchhoff-Love plate theory ($\varepsilon_z = \gamma_{yz} = \gamma_{zx} = 0$). So, transverse stresses and strains are not considered. Acceptable results are only predicted for thin laminates, where the smallest system length is significantly larger than the laminate thickness. This effect is particularly pronounced in composites because the shear moduli G_{zx}, G_{yz} of most of the composites are relatively small compared with those of isotropic plate materials.

Effects of temperature and moisture induced strains and stresses are not included here.

Background information about laminates, composites and the respective theories can be found in the literature (e.g. Refs. [1, 2, 3]).

The Classical Laminate Theory has been developed for plane plates, but it may be used for slightly curved plates or shallow shells as well.

2 List of Symbols

Symbol	Unit	Description
$[a]$	mm/N	extensional sub-matrix of the inverse laminate stiffness matrix
$[b]$	$1/\mathrm{N}$	coupling sub-matrix of the inverse laminate stiffness matrix
$[d]$	$1/(\mathrm{N}\cdot\mathrm{mm})$	flexural sub-matrix of the inverse laminate stiffness matrix
ℓ	mm	smallest system length
m	$\mathrm{N}\cdot\mathrm{mm}/\mathrm{mm}$	section moment (bending stress resultant per unit length or width)
n	–	total number of layers
n^0	N/mm	section force (membrane stress resultant per unit length or width)
t, t_k	mm	laminate thickness, thickness of the k^{th} layer
u, v	mm	membrane displacements
w	mm	deflection
x_1, x_2	mm	layer coordinate system
x, y, z	mm	laminate coordinate system
$[A]$	N/mm	extensional stiffness matrix of laminate (membrane stretching matrix)
$[B]$	N	coupling stiffness matrix of laminate (bending-stretching matrix)
$[D]$	$\mathrm{N}\cdot\mathrm{mm}$	flexural stiffness matrix of laminate (bending stiffness matrix)
E	MPa	Young's Modulus
G	MPa	shear modulus
$[K]$	N/mm, N, $\mathrm{N}\cdot\mathrm{mm}$	laminate stiffness matrix (ABD-matrix)
$[Q]_k$	MPa	reduced stiffness matrix (2D) of single layer k in layer coordinates
$[Q']_k$	MPa	reduced stiffness matrix (2D) of single layer k in laminate coordinates
$[S]_k$	$1/\mathrm{MPa}$	compliance matrix (2D) of single layer k in layer coordinates
$[T_\sigma]_k$, $[T_\varepsilon]_k$	–	stress and strain transformation matrices for the single layer k
α	$^\circ$	layer orientation angle
γ	$^\circ/^\circ$	shear strain
ε	mm/mm	normal strain
κ_x, κ_y	$1/\mathrm{mm}$	curvature
κ_{xy}	$1/\mathrm{mm}$	twist
ν	–	Poisson's ratio
φ	–	fiber volume fraction
σ	MPa	normal stress
τ	MPa	shear stress

Indices	Description
^{0}	related to the reference surface
$_{1,2}$	related to the layer coordinate axes
$_{f,m}$	fiber material, matrix material
$_{i,j}$	general indices
$_k$	layer number of single layer
$_{x,y,z}$	related to the laminate coordinate axes
$'$	in the laminate coordinate system
$_{\perp,\parallel,\#}$	symbolic denotation for quantities of unidirectional layers

Note: The matrices $[A]$, $[B]$, $[D]$, $[Q]_k$, $[Q']_k$ and $[S]_k$ are symmetric 3×3-matrices. Their elements follow the numbering scheme

$$\begin{bmatrix} A_{11} & A_{12} & A_{16} \\ A_{12} & A_{22} & A_{26} \\ A_{16} & A_{26} & A_{66} \end{bmatrix}$$

Elements containing the indices 3, 4 or 5 are spared for 3D problems.

3 Analysis

3.1 Prerequisites

The Classical Laminate Theory includes the thin plate theory of Kirchhoff-Love which – originally developed for isotropic material – is expanded to laminates with anisotropic material behaviour.
The following prerequisites are made:

- Each layer is macroscopically homogeneous and can be treated as a homogenized material.
- The layers are ideally bonded, there exist no gaps or cavities.
- The stress-strain relationship follows the generalized Hooke's law, stresses and strains are proportional.
- The laminate thickness t is small with respect to other dimensions and the transverse deflection of the reference surface is small compared to t.
- An initially straight line perpendicular to the reference surface remains straight and perpendicular to the reference surface during deformation (Euler-Bernoulli hypothesis).
- Displacements perpendicular to the reference surface do not depend on the z-coordinate.

From these presumptions, it follows that transverse stresses and strains (σ_z, τ_{yz}, τ_{zx}, ε_z, γ_{yz}, γ_{zx}) vanish and that strains parallel to the surfaces (ε_x, ε_y, γ_{xy}) are linearly distributed over the laminate thickness. Stresses parallel to the surfaces (σ_x, σ_y, τ_{xy}) are linearly distributed over the thickness of the single layers but may have discontinuities at the layer boundary surfaces.

An overview over the configuration, coordination systems, stresses and strains is given in Fig. 1.

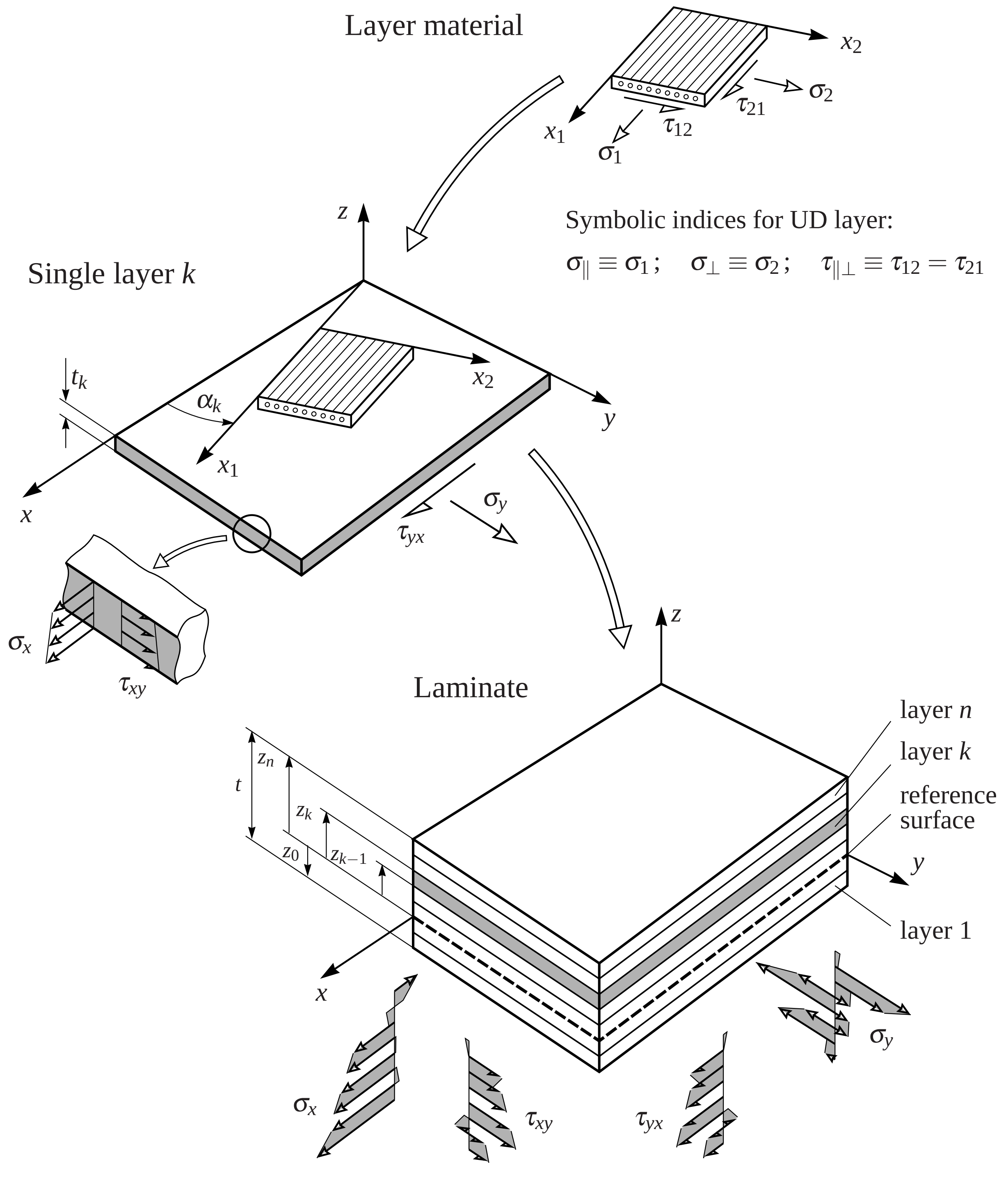

Figure 1: Layer material – Single layer – Laminate

3.2 Stress-strain relationship of a single layer

3.2.1 Layer coordinate system

Stresses and strains are described in a layer coordinate system with the axes x_1, x_2. It is assumed that the layer material behaves orthotropically (meaning that main material axes are perpendicular to each other) and the coordinate axes x_1 and x_2 are chosen parallel to the material's orthotropy axes.

Stress and strain vectors for the k^{th} layer read

$$\{\sigma\}_k = \left\{ \begin{array}{c} \sigma_1 \\ \sigma_2 \\ \tau_{12} \end{array} \right\}_k ; \qquad \{\varepsilon\}_k = \left\{ \begin{array}{c} \varepsilon_1 \\ \varepsilon_2 \\ \gamma_{12} \end{array} \right\}_k \tag{1}$$

The strain-stress relationship and the stress-strain relationship are

$$\{\varepsilon\}_k = [S]_k \cdot \{\sigma\}_k ; \qquad \{\sigma\}_k = [Q]_k \cdot \{\varepsilon\}_k \tag{2}$$

with the compliance matrix $[S]_k$ and the reduced stiffness matrix $[Q]_k$ which are derived from the material's elasticity constants

$$[S]_k = \begin{bmatrix} \frac{1}{E_1} & \frac{-\nu_{21}}{E_2} & 0 \\ \frac{-\nu_{12}}{E_1} & \frac{1}{E_2} & 0 \\ 0 & 0 & \frac{1}{G_{12}} \end{bmatrix}_k ; \qquad [Q]_k = [S]_k^{-1} = \begin{bmatrix} \frac{E_1}{1-\nu_{12}\cdot\nu_{21}} & \frac{\nu_{21}\cdot E_1}{1-\nu_{12}\cdot\nu_{21}} & 0 \\ \frac{\nu_{12}\cdot E_2}{1-\nu_{12}\cdot\nu_{21}} & \frac{E_2}{1-\nu_{12}\cdot\nu_{21}} & 0 \\ 0 & 0 & G_{12} \end{bmatrix}_k \tag{3}$$

Compliance and stiffness matrices are symmetric and the Maxwell-Betti formula holds

$$\frac{\nu_{12}}{E_1} = \frac{\nu_{21}}{E_2} \tag{4}$$

meaning that there are only four independent elasticity constants E_1, E_2, ν_{12} and G_{12}.

The Poisson's ratio ν_{ij} is used such that i indicates the action – i.e. the direction of the driving stress – and j indicates the reaction – i.e. the direction of the corresponding lateral contraction.

Note: In Eq. (3), the indexing of the Poisson's ratio does not coincide with the mathematical convention for the matrix element indices (e.g. $S_{12} = -\nu_{21}/E_2$). And one should be aware that another convention for the indexing of the Poisson's ratio is also used in the literature (refer to [4]).

It is common practice to choose the coordinate system such that $E_1 > E_2$ and $\nu_{12} > \nu_{21}$. For fiber reinforced unidirectional layers, symbolic indices may be used with the equivalence

$$E_{\parallel} \equiv E_1 ; \quad E_{\perp} \equiv E_2 ; \quad \nu_{\parallel\perp} \equiv \nu_{12} ; \quad G_{\#} \equiv G_{12} \tag{5}$$

The constants above are determined by tests and - if micro-mechanical properties for the constituents are available - may be assessed with associated micro-mechanical formulas.
Usually, ν_{12} is the larger Poisson's ratio and can be more accurately measured than ν_{21}.

3.2.2 Laminate coordinate system

The laminate uses a right hand coordinate system x, y, z with its origin at the reference surface which is common for all layers. The x- and y-axes lie in the reference surface, their orientation may be chosen arbitrarily. The z-axis is normal to the reference surface. The position of the reference surface may be arbitrary, but usually the mid-surface of the laminate is taken.

The orientation of each single layer is described by an angle α_k which is defined as the rotation angle from the x-axis (laminate coordination system) to the x_1-axis (layer coordinate system). α_k is positive in the counter clockwise direction (see Fig. 1).

Stress and strain vectors for the k^{th} layer in the laminate coordination system read

$$\{\sigma'\}_k = \left\{ \begin{array}{c} \sigma_x \\ \sigma_y \\ \tau_{xy} \end{array} \right\}_k ; \qquad \{\varepsilon'\}_k = \left\{ \begin{array}{c} \varepsilon_x \\ \varepsilon_y \\ \gamma_{xy} \end{array} \right\}_k \tag{6}$$

and are derived from $\{\sigma\}_k$ and $\{\varepsilon\}_k$ by

$$\{\sigma'\}_k = [T_\sigma]_k \cdot \{\sigma\}_k \,; \qquad \{\varepsilon'\}_k = [T_\varepsilon]_k \cdot \{\varepsilon\}_k \tag{7}$$

with the transformation matrices

$$[T_\sigma]_k = \begin{bmatrix} \cos^2(\alpha) & \sin^2(\alpha) & -2\cdot\sin(\alpha)\cdot\cos(\alpha) \\ \sin^2(\alpha) & \cos^2(\alpha) & 2\cdot\sin(\alpha)\cdot\cos(\alpha) \\ \sin(\alpha)\cdot\cos(\alpha) & -\sin(\alpha)\cdot\cos(\alpha) & \cos^2(\alpha)-\sin^2(\alpha) \end{bmatrix}_k \tag{8}$$

$$[T_\varepsilon]_k = \begin{bmatrix} \cos^2(\alpha) & \sin^2(\alpha) & -\sin(\alpha)\cdot\cos(\alpha) \\ \sin^2(\alpha) & \cos^2(\alpha) & \sin(\alpha)\cdot\cos(\alpha) \\ 2\cdot\sin(\alpha)\cdot\cos(\alpha) & -2\cdot\sin(\alpha)\cdot\cos(\alpha) & \cos^2(\alpha)-\sin^2(\alpha) \end{bmatrix}_k \tag{9}$$

The transformation matrices are related to each other by the condition $[T_\sigma]_k^T = [T_\varepsilon]_k^{-1}$. The inverse transformation matrices can be simply obtained if the angle α is replaced by $-\alpha$ because the inverse transformation just means a rotation of the same amount into the opposite direction.

The transformed reduced stiffness matrix reads

$$[Q']_k = [T_\sigma]_k \cdot [Q]_k \cdot [T_\sigma]_k^T \tag{10}$$

The elements of this matrix can be calculated in a compact form (the index k has been omitted for brevity) as

$$\begin{aligned}
Q'_{11} &= Q_{11}\cdot\cos^4(\alpha) + 2\cdot(Q_{12}+2\cdot Q_{66})\cdot\sin^2(\alpha)\cdot\cos^2(\alpha) + Q_{22}\cdot\sin^4(\alpha) \\
Q'_{12} &= (Q_{11}+Q_{22}-4\cdot Q_{66})\cdot\sin^2(\alpha)\cdot\cos^2(\alpha) + Q_{12}\cdot\left[\sin^4(\alpha)+\cos^4(\alpha)\right] \\
Q'_{22} &= Q_{11}\cdot\sin^4(\alpha) + 2\cdot(Q_{12}+2\cdot Q_{66})\cdot\sin^2(\alpha)\cdot\cos^2(\alpha) + Q_{22}\cdot\cos^4(\alpha) \\
Q'_{16} &= (Q_{11}-Q_{12}-2\cdot Q_{66})\cdot\sin(\alpha)\cdot\cos^3(\alpha) + (Q_{12}-Q_{22}+2\cdot Q_{66})\cdot\sin^3(\alpha)\cdot\cos(\alpha) \\
Q'_{26} &= (Q_{11}-Q_{12}-2\cdot Q_{66})\cdot\sin^3(\alpha)\cdot\cos(\alpha) + (Q_{12}-Q_{22}+2\cdot Q_{66})\cdot\sin(\alpha)\cdot\cos^3(\alpha) \\
Q'_{66} &= (Q_{11}+Q_{22}-2\cdot Q_{12}-2\cdot Q_{66})\cdot\sin^2(\alpha)\cdot\cos^2(\alpha) + Q_{66}\cdot\left[\sin^4(\alpha)+\cos^4(\alpha)\right]
\end{aligned} \tag{11}$$

The stress-strain relationship in the laminate coordinate system reads

$$\{\sigma'\}_k = [Q']_k \cdot \{\varepsilon'\}_k \tag{12}$$

3.3 Constitutive equations of the laminate

The laminate considered is a thin structure (a plane plate, a slightly curved plate or a shallow shell) with a plane stress state. It consists of n layers each having a constant thickness t_k. The orientation of each individual layer is described by the angle α_k.

The strain vector (common for all layers) is written as

$$\{\varepsilon'\} = \{\varepsilon^0\} + z\cdot\{\kappa\} \tag{13}$$

where $\{\varepsilon^0\}$ represents the strain in the reference surface and $\{\kappa\}$ its curvature. $\{\varepsilon^0\}$ and $\{\kappa\}$ depend only on the x-y-position.

The strain vector $\{\varepsilon^0\}$ is linked to the displacements u^0 and v^0 and the curvature vector $\{\kappa\}$ to the deflection w^0 of the reference surface via

$$\{\varepsilon^0\} = \begin{Bmatrix} \varepsilon_x^0 \\ \varepsilon_y^0 \\ \gamma_{xy}^0 \end{Bmatrix} = \begin{Bmatrix} \frac{\partial u^0}{\partial x} \\ \frac{\partial v^0}{\partial y} \\ \frac{\partial u^0}{\partial y} + \frac{\partial v^0}{\partial x} \end{Bmatrix}; \qquad \{\kappa\} = \begin{Bmatrix} \kappa_x \\ \kappa_y \\ \kappa_{xy} \end{Bmatrix} = \begin{Bmatrix} -\frac{\partial^2 w^0}{\partial x^2} \\ -\frac{\partial^2 w^0}{\partial y^2} \\ -2\cdot\frac{\partial^2 w^0}{\partial x\cdot\partial y} \end{Bmatrix} \tag{14}$$

Details of the laminate deformation are shown in Fig. 2.

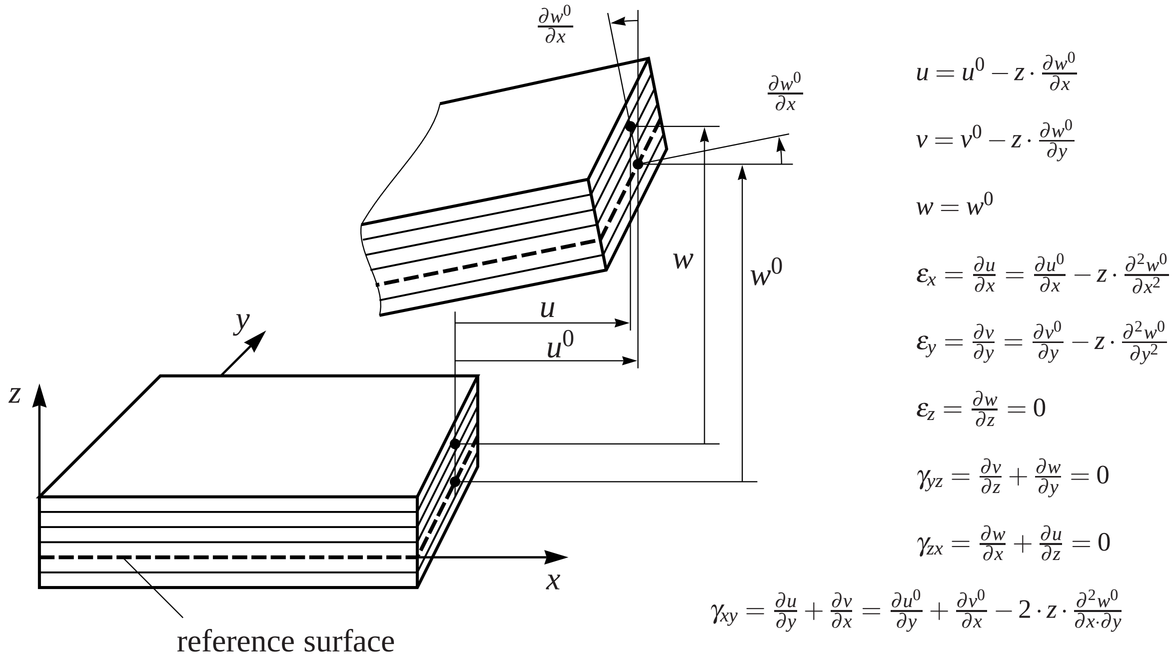

Figure 2: Laminate deformation (based on the Kirchhoff-Love plate theory)

The vectors of section forces $\{n^0\}$ and of section moments $\{m\}$ are obtained integrating the stresses over the plate thickness leading to

$$\{n^0\} = \left\{ \begin{array}{c} n_x^0 \\ n_y^0 \\ n_{xy}^0 \end{array} \right\} = \int_{-t/2}^{t/2} \{\sigma'\} \cdot \mathrm{d}z = \sum_{k=1}^{n} \int_{z_{k-1}}^{z_k} \{\sigma'\}_k \cdot \mathrm{d}z \tag{15}$$

$$\{m\} = \left\{ \begin{array}{c} m_x \\ m_y \\ m_{xy} \end{array} \right\} = \int_{-t/2}^{t/2} \{\sigma'\} \cdot z \cdot \mathrm{d}z = \sum_{k=1}^{n} \int_{z_{k-1}}^{z_k} \{\sigma'\}_k \cdot z \cdot \mathrm{d}z \tag{16}$$

where it is assumed for the section moments in Eq. (16) that the section forces according to Eq. (15) act in the reference surface.

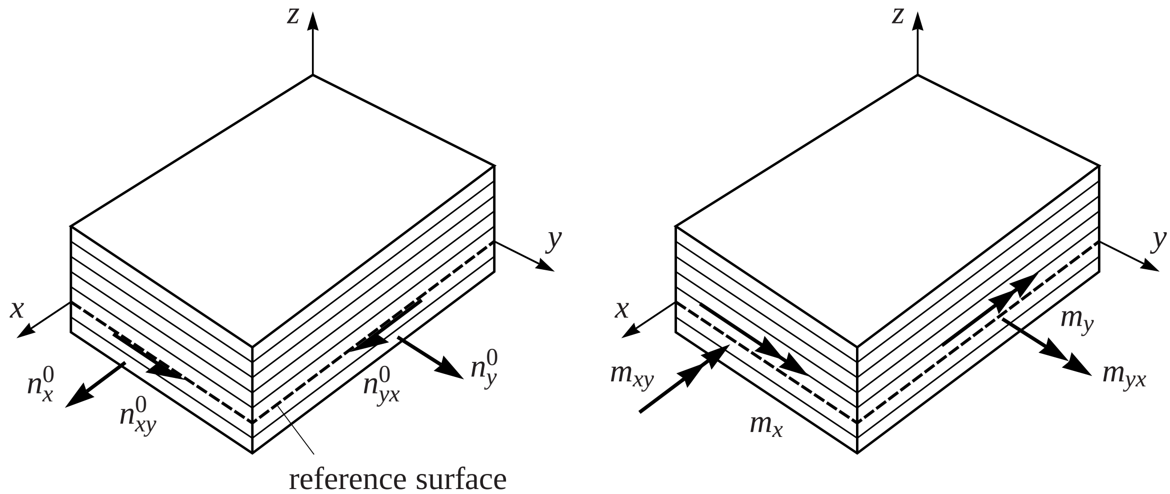

Figure 3: Laminate section forces and section moments

Eqs. (13) and (12) are inserted into Eqs. (15) and (16) and the matrices $[A]$ (extensional stiffness matrix), $[B]$ (coupling stiffness matrix) and $[D]$ (flexural stiffness matrix) – which evaluate the integration above – are introduced

$$\begin{aligned}
[A] &= \sum_{k=1}^{n} \left[Q'\right]_k \cdot (z_k - z_{k-1}) \\
[B] &= \sum_{k=1}^{n} \left[Q'\right]_k \cdot \frac{z_k^2 - z_{k-1}^2}{2} \\
[D] &= \sum_{k=1}^{n} \left[Q'\right]_k \cdot \frac{z_k^3 - z_{k-1}^3}{3}
\end{aligned} \tag{17}$$

The matrices $[A]$, $[B]$ and $[D]$ can be combined to the laminate stiffness matrix

$$[K] = \begin{bmatrix} [A] & [B] \\ [B] & [D] \end{bmatrix} \tag{18}$$

and the section forces and moments are expressed as

$$\left\{ \begin{array}{c} \{n^0\} \\ \{m\} \end{array} \right\} = \begin{bmatrix} [A] & [B] \\ [B] & [D] \end{bmatrix} \cdot \left\{ \begin{array}{c} \{\varepsilon^0\} \\ \{\kappa\} \end{array} \right\} = [K] \cdot \left\{ \begin{array}{c} \{\varepsilon^0\} \\ \{\kappa\} \end{array} \right\} \tag{19}$$

For a laminate symmetric to its reference surface, the coupling stiffness matrix $[B]$ vanishes. The membrane problem and the bending problem can be separately treated with the simplified formulas

$$\{n^0\} = [A] \cdot \{\varepsilon^0\} \quad \text{and} \quad \{m\} = [D] \cdot \{\kappa\} \tag{20}$$

If the loading is known, one can obtain the unknown strains and curvatures from

$$\left\{ \begin{array}{c} \{\varepsilon^0\} \\ \{\kappa\} \end{array} \right\} = [K]^{-1} \cdot \left\{ \begin{array}{c} \{n^0\} \\ \{m\} \end{array} \right\} \tag{21}$$

The inverse laminate stiffness matrix $[K]^{-1}$ is subdivided into the sub-matrices $[a]$, $[b]$ and $[d]$ to

$$[K]^{-1} = \begin{bmatrix} [a] & [b] \\ [b]^T & [d] \end{bmatrix} \tag{22}$$

where $[a]$ and $[d]$ are symmetric 3×3-matrices. But the sub-matrix $[b]$ is not symmetric ($[b] \neq [b]^T$). In the general case, where the coupling stiffness matrix does not vanish ($[B] \neq 0$), the sub-matrices $[a]$, $[b]$ and $[d]$ can be directly obtained as

$$\begin{aligned}
[a] &= \Big([A] - [B] \cdot [D]^{-1} \cdot [B]\Big)^{-1} \\
[b] &= \Big([B] - [D] \cdot [B]^{-1} \cdot [A]\Big)^{-1} \\
[d] &= \Big([D] - [B] \cdot [A]^{-1} \cdot [B]\Big)^{-1}
\end{aligned} \tag{23}$$

If the coupling stiffness matrix vanishes ($[B] = 0$), the sub-matrix $[b]$ can not be calculated in this way and the Eqs. (23) are replaced by

$$[a] = [A]^{-1}; \quad [b] = [b]^T = 0; \quad [d] = [D]^{-1} \tag{24}$$

For practical application, it might not be necessary to invert the laminate stiffness matrix $[K]$ to determine the laminate compliance matrix $[K]^{-1}$, but it could be more convenient to only solve the equation systems (19) or (20), respectively.

3.4 Layer strains and stresses

For strength analyses, the so-called natural strains and stresses in the layer coordinate system are required. The strains in the k^{th} layer are derived from Eqs. (7) and (13) yielding

$$\{\varepsilon\}_k = [T_\varepsilon]_k^{-1} \cdot \{\varepsilon'\}_k = [T_\sigma]_k^T \cdot \left(\{\varepsilon^0\} + z \cdot \{\kappa\}\right) \tag{25}$$

with z in the range $z_{k-1} \leq z \leq z_k$.

Stresses in the k^{th} layer are predicted with Eq. (2) to

$$\{\sigma\}_k = [Q]_k \cdot \{\varepsilon\}_k \tag{26}$$

4 Example

Task:

Predict the laminate stiffness matrix as well as the strains and stresses in a composite plate strip.

Given:

The investigated configuration is a laminate $[0/10/90/70]$ with a thickness of $t = 0.5\,\text{mm}$ and with a thickness of each layer of $t_k = 0.125\,\text{mm}$. The reference surface shall be the mid-plane of the laminate. For the single CFRP/epoxy layer of the stack the following properties are given with symbolic suffixes according to Eq. (5):

$E_{\|\|}$	$E_\perp$	$G_\#$	$\nu_{\|\|\perp}$
MPa	MPa	MPa	–
132 700	9 300	4 600	0.28

Loading in terms of section forces and section moments is given as

$$\{n^0\} = \begin{Bmatrix} 100 \\ 125 \\ 80 \end{Bmatrix} \text{N/mm} \quad \text{and} \quad \{m\} = \begin{Bmatrix} 15 \\ 20 \\ 12 \end{Bmatrix} \text{N}\cdot\text{mm/mm}$$

Computation:

Note: Calculations for the investigated example have been done numerically with a given internal parameter resolution. For convenience, the results are given in a rounded format. This means that a restart of the calculation from a rounded intermediate result may lead to subsequent deviations from the presented data.

The stiffness matrices of the material in the layer coordinate systems are computed with Eq. (3)

$$[Q]_1 = [Q]_2 = [Q]_3 = [Q]_4 = \begin{bmatrix} 133\,433 & 2\,618 & 0 \\ 2\,618 & 9\,351 & 0 \\ 0 & 0 & 4\,600 \end{bmatrix} \text{MPa}$$

Transformation into the laminate coordinate system is done with Eqs. (11). However, the transformation matrices $[T_\sigma]_k$ according to Eq. (8) are given as well

$$[T_\sigma]_1 = \begin{bmatrix} 1 & 0 & 0 \\ 0 & 1 & 0 \\ 0 & 0 & 1 \end{bmatrix}; \qquad [Q']_1 = \begin{bmatrix} 133\,433 & 2\,618 & 0 \\ 2\,618 & 9\,351 & 0 \\ 0 & 0 & 4\,600 \end{bmatrix} \text{MPa}$$

$$[T_\sigma]_2 = \begin{bmatrix} 0.9699 & 0.0302 & -0.3420 \\ 0.0302 & 0.9699 & 0.3420 \\ 0.1710 & -0.1710 & 0.9397 \end{bmatrix}; \qquad [Q']_2 = \begin{bmatrix} 126\,207 & 6\,103 & 20\,183 \\ 6\,103 & 9\,608 & 1\,036 \\ 20\,183 & 1\,036 & 8\,084 \end{bmatrix} \text{MPa}$$

$$[T_\sigma]_3 = \begin{bmatrix} 0 & 1 & 0 \\ 1 & 0 & 0 \\ 0 & 0 & -1 \end{bmatrix}; \qquad [Q']_3 = \begin{bmatrix} 9\,351 & 2\,618 & 0 \\ 2\,618 & 133\,433 & 0 \\ 0 & 0 & 4\,600 \end{bmatrix} \text{MPa}$$

$$[T_\sigma]_4 = \begin{bmatrix} 0.1170 & 0.8830 & -0.6428 \\ 0.8830 & 0.1170 & 0.6428 \\ 0.3214 & -0.3214 & -0.7660 \end{bmatrix}; \qquad [Q']_4 = \begin{bmatrix} 11\,559 & 14\,926 & 5\,272 \\ 14\,926 & 106\,611 & 34\,607 \\ 5\,272 & 34\,607 & 16\,907 \end{bmatrix} \text{MPa}$$

This leads to the laminate stiffness matrix (refer to Eqs. (17) and (18))

$$[K] = \begin{bmatrix} [A] & [B] \\ [B] & [D] \end{bmatrix} = \begin{bmatrix} 35\,069 & 3\,283 & 3\,182 & -3\,769 & 261 & -34 \\ 3\,283 & 32\,376 & 4\,455 & 261 & 3\,247 & 803 \\ 3\,182 & 4\,455 & 4\,274 & -34 & 803 & 261 \\ -3\,769 & 261 & -34 & 749 & 86 & 37 \\ 261 & 3\,247 & 803 & 86 & 622 & 158 \\ -34 & 803 & 261 & 37 & 158 & 106 \end{bmatrix}$$

with $[A]$ in N/mm, $[B]$ in N and $[D]$ in N·mm, and its inverse

$$[K]^{-1} = \begin{bmatrix} [a] & [b] \\ [b]^T & [d] \end{bmatrix} = \begin{bmatrix} 7.22 & -0.37 & -4.82 & 36.09 & -1.53 & 6.63 \\ -0.37 & 6.54 & -0.25 & -0.36 & -34.16 & 2.15 \\ -4.82 & -0.25 & 34.96 & -17.37 & -30.89 & -33.44 \\ 36.09 & -0.36 & -17.37 & 318.54 & -33.64 & -4.25 \\ -1.53 & -34.16 & -30.89 & -33.64 & 478.03 & -367.15 \\ 6.63 & 2.15 & -33.44 & -4.25 & -367.15 & 1\,557.74 \end{bmatrix} \cdot 10^{-5}$$

with $[a]$ in mm/N, $[b]$ in 1/N and $[d]$ in $1/(\text{N}\cdot\text{mm})$, respectively.

Vectors of strain and curvature in the reference surface are obtained by solving Eq. (19). However, they may be determined with Eq. (21) instead.

$$\{\varepsilon^0\} = \begin{Bmatrix} 8.81 \\ 0.97 \\ 10.03 \end{Bmatrix} \cdot 10^{-3}\,\text{mm/mm}; \qquad \{\kappa\} = \begin{Bmatrix} 62.29 \\ -22.44 \\ 95.42 \end{Bmatrix} \cdot 10^{-3}/\text{mm}$$

The strains ε_x, ε_y and γ_{xy} at the layer boundary surfaces can be calculated with Eq. (13).
The strains $\varepsilon_\parallel$, $\varepsilon_\perp$ and $\gamma_{\parallel\perp}$ at the layer boundary surfaces are calculated with Eq. (25).
Stresses $\sigma_\parallel$, $\sigma_\perp$ and $\tau_{\parallel\perp}$ at the layer boundary surfaces are predicted with Eq. (26).

Laminate loading, strain and curvature as well as layer strains and stresses are summarized in the following tables.

All section forces and moments:

n_x^0	in N/mm		100						
n_y^0	in N/mm		125						
n_{xy}^0	in N/mm		80						
m_x	in N·mm/mm		15						
m_y	in N·mm/mm		20						
m_{xy}	in N·mm/mm		12						
ε_x^0	in 10^{-3} mm/mm		8.81						
ε_y^0	in 10^{-3} mm/mm		0.97						
γ_{xy}^0	in 10^{-3} °/°		10.03						
κ_x	in 10^{-3}/mm		62.29						
κ_y	in 10^{-3}/mm		−22.44						
κ_{xy}	in 10^{-3}/mm		95.42						
		layer 1		layer 2		layer 3		layer 4	
α	in °	0		10		90		70	
z	in mm	−0.25	−0.125	−0.125	0.0	0.0	0.125	0.125	0.25
ε_x	in 10^{-3} mm/mm	−6.77	1.02	1.02	8.81	8.81	16.59	16.59	24.38
ε_y	in 10^{-3} mm/mm	6.58	3.77	3.77	0.97	0.97	−1.84	−1.84	−4.64
γ_{xy}	in 10^{-3} °/°	−13.82	−1.89	−1.89	10.03	10.03	21.96	21.96	33.89
$\varepsilon_{\parallel}$	in 10^{-3} mm/mm	−6.77	1.02	0.78	10.28	0.97	−1.84	7.38	9.64
$\varepsilon_{\perp}$	in 10^{-3} mm/mm	6.58	3.77	4.01	−0.51	8.81	16.59	7.38	10.09
$\gamma_{\parallel\perp}$	in 10^{-3} °/°	−13.82	−1.89	−0.84	6.75	−10.03	−21.96	−28.67	−44.61
$\sigma_{\parallel}$	in MPa	−885.7	145.9	114.4	1 371.0	152.3	−201.6	1 003.7	1 313.3
$\sigma_{\perp}$	in MPa	43.8	38.0	39.6	22.2	84.9	150.3	88.3	119.6
$\tau_{\parallel\perp}$	in MPa	−63.6	−8.7	−3.9	31.0	−46.2	−101.0	−131.9	−205.2

Only section normal force n_x^0:

n_x^0	in N/mm	100							
n_y^0	in N/mm	0							
n_{xy}^0	in N/mm	0							
m_x	in N·mm/mm	0							
m_y	in N·mm/mm	0							
m_{xy}	in N·mm/mm	0							
ε_x^0	in 10^{-3} mm/mm	7.22							
ε_y^0	in 10^{-3} mm/mm	−0.37							
γ_{xy}^0	in 10^{-3} °/°	−4.82							
κ_x	in 10^{-3}/mm	36.09							
κ_y	in 10^{-3}/mm	−1.53							
κ_{xy}	in 10^{-3}/mm	6.63							
		layer 1		layer 2		layer 3		layer 4	
α	in °	0		10		90		70	
z	in mm	−0.25	−0.125	−0.125	0.0	0.0	0.125	0.125	0.25
ε_x	in 10^{-3} mm/mm	−1.80	2.71	2.71	7.22	7.22	11.73	11.73	16.24
ε_y	in 10^{-3} mm/mm	0.01	−0.18	−0.18	−0.37	−0.37	−0.56	−0.56	−0.75
γ_{xy}	in 10^{-3} °/°	−6.47	−5.65	−5.65	−4.82	−4.82	−3.99	−3.99	−3.16
$\varepsilon_{\parallel}$	in 10^{-3} mm/mm	−1.80	2.71	1.66	6.17	−0.37	−0.56	−0.41	0.22
$\varepsilon_{\perp}$	in 10^{-3} mm/mm	0.01	−0.18	0.87	0.68	7.22	11.73	11.58	15.27
$\gamma_{\parallel\perp}$	in 10^{-3} °/°	−6.47	−5.65	−6.29	−7.12	4.82	3.99	−4.85	−8.50
$\sigma_{\parallel}$	in MPa	−240.5	361.0	223.3	824.8	−30.6	−44.4	−24.0	69.1
$\sigma_{\perp}$	in MPa	−4.6	5.4	12.5	22.5	66.6	108.2	107.2	143.4
$\tau_{\parallel\perp}$	in MPa	−29.8	−26.0	−29.0	−32.8	22.2	18.4	−22.3	−39.1

Only section normal force n_y^0:

n_x^0	in N/mm	0							
n_y^0	in N/mm	125							
n_{xy}^0	in N/mm	0							
m_x	in N·mm/mm	0							
m_y	in N·mm/mm	0							
m_{xy}	in N·mm/mm	0							
ε_x^0	in 10^{-3} mm/mm	−0.46							
ε_y^0	in 10^{-3} mm/mm	8.17							
γ_{xy}^0	in 10^{-3} °/°	−0.32							
κ_x	in 10^{-3}/mm	−0.45							
κ_y	in 10^{-3}/mm	−42.70							
κ_{xy}	in 10^{-3}/mm	2.69							
		layer 1		layer 2		layer 3		layer 4	
α	in °	0		10		90		70	
z	in mm	−0.25	−0.125	−0.125	0.0	0.0	0.125	0.125	0.25
ε_x	in 10^{-3} mm/mm	−0.35	−0.41	−0.41	−0.46	−0.46	−0.52	−0.52	−0.58
ε_y	in 10^{-3} mm/mm	18.84	13.51	13.51	8.17	8.17	2.83	2.83	−2.50
γ_{xy}	in 10^{-3} °/°	−0.99	−0.65	−0.65	−0.32	−0.32	0.02	0.02	0.35
$\varepsilon_{\parallel}$	in 10^{-3} mm/mm	−0.35	−0.41	−0.10	−0.26	8.17	2.83	2.45	−2.16
$\varepsilon_{\perp}$	in 10^{-3} mm/mm	18.84	13.51	13.20	7.96	−0.46	−0.52	−0.13	−0.92
$\gamma_{\parallel\perp}$	in 10^{-3} °/°	−0.99	−0.65	4.14	2.65	0.32	−0.02	2.14	−1.51
$\sigma_{\parallel}$	in MPa	2.5	−19.0	21.2	−13.6	1 089.0	376.8	326.2	−291.2
$\sigma_{\perp}$	in MPa	175.3	125.2	123.2	73.8	17.1	2.6	5.2	−14.2
$\tau_{\parallel\perp}$	in MPa	−4.6	−3.0	19.1	12.2	1.5	−0.1	9.9	−6.9

Only section shear force n_{xy}^0:

n_x^0	in N/mm	0							
n_y^0	in N/mm	0							
n_{xy}^0	in N/mm	80							
m_x	in N·mm/mm	0							
m_y	in N·mm/mm	0							
m_{xy}	in N·mm/mm	0							
ε_x^0	in 10^{-3} mm/mm	-3.85							
ε_y^0	in 10^{-3} mm/mm	-0.20							
γ_{xy}^0	in 10^{-3} °/°	27.97							
κ_x	in 10^{-3}/mm	-13.90							
κ_y	in 10^{-3}/mm	-24.71							
κ_{xy}	in 10^{-3}/mm	-26.75							
		layer 1		layer 2		layer 3		layer 4	
α	in °	0		10		90		70	
z	in mm	-0.25	-0.125	-0.125	0.0	0.0	0.125	0.125	0.25
ε_x	in 10^{-3} mm/mm	-0.38	-2.12	-2.12	-3.85	-3.85	-5.59	-5.59	-7.33
ε_y	in 10^{-3} mm/mm	5.97	2.89	2.89	-0.20	-0.20	-3.29	-3.29	-6.38
γ_{xy}	in 10^{-3} °/°	34.65	31.31	31.31	27.97	27.97	24.62	24.62	21.28
$\varepsilon_{\parallel}$	in 10^{-3} mm/mm	-0.38	-2.12	3.39	1.04	-0.20	-3.29	4.35	0.35
$\varepsilon_{\perp}$	in 10^{-3} mm/mm	5.97	2.89	-2.62	-5.10	-3.85	-5.59	-13.24	-14.06
$\gamma_{\parallel\perp}$	in 10^{-3} °/°	34.65	31.31	31.13	27.53	-27.97	-24.62	-17.39	-15.69
$\sigma_{\parallel}$	in MPa	-35.0	-274.9	445.3	125.2	-37.3	-454.0	546.0	9.4
$\sigma_{\perp}$	in MPa	54.9	21.4	-15.6	-44.9	-36.6	-60.9	-112.4	-130.6
$\tau_{\parallel\perp}$	in MPa	159.4	144.0	143.2	126.6	-128.6	-113.3	-80.0	-72.2

Only section bending moment m_x:

n_x^0	in N/mm	0							
n_y^0	in N/mm	0							
n_{xy}^0	in N/mm	0							
m_x	in N·mm/mm	15							
m_y	in N·mm/mm	0							
m_{xy}	in N·mm/mm	0							
ε_x^0	in 10^{-3} mm/mm	5.41							
ε_y^0	in 10^{-3} mm/mm	−0.05							
γ_{xy}^0	in 10^{-3} °/°	−2.61							
κ_x	in 10^{-3}/mm	47.78							
κ_y	in 10^{-3}/mm	−5.05							
κ_{xy}	in 10^{-3}/mm	−0.64							
		layer 1		layer 2		layer 3		layer 4	
α	in °	0		10		90		70	
z	in mm	−0.25	−0.125	−0.125	0.0	0.0	0.125	0.125	0.25
ε_x	in 10^{-3} mm/mm	−6.53	−0.56	−0.56	5.41	5.41	11.39	11.39	17.36
ε_y	in 10^{-3} mm/mm	1.21	0.58	0.58	−0.05	−0.05	−0.68	−0.68	−1.32
γ_{xy}	in 10^{-3} °/°	−2.45	−2.53	−2.53	−2.61	−2.61	−2.69	−2.69	−2.77
$\varepsilon_{\parallel}$	in 10^{-3} mm/mm	−6.53	−0.56	−0.96	4.80	−0.05	−0.68	−0.14	−0.02
$\varepsilon_{\perp}$	in 10^{-3} mm/mm	1.21	0.58	0.97	0.56	5.41	11.39	10.84	16.06
$\gamma_{\parallel\perp}$	in 10^{-3} °/°	−2.45	−2.53	−1.99	−4.32	2.61	2.69	−5.70	−9.89
$\sigma_{\parallel}$	in MPa	−868.3	−73.0	−125.0	642.4	7.0	−61.6	10.2	39.4
$\sigma_{\perp}$	in MPa	−5.8	3.9	6.6	17.8	50.5	104.7	101.0	150.2
$\tau_{\parallel\perp}$	in MPa	−11.3	−11.6	−9.1	−19.9	12.0	12.4	−26.2	−45.5

Only section bending moment m_y:

n_x^0	in N/mm		0						
n_y^0	in N/mm		0						
n_{xy}^0	in N/mm		0						
m_x	in N·mm/mm		0						
m_y	in N·mm/mm		20						
m_{xy}	in N·mm/mm		0						
ε_x^0	in 10^{-3} mm/mm		-0.31						
ε_y^0	in 10^{-3} mm/mm		-6.83						
γ_{xy}^0	in 10^{-3} °/°		-6.18						
κ_x	in 10^{-3}/mm		-6.73						
κ_y	in 10^{-3}/mm		95.61						
κ_{xy}	in 10^{-3}/mm		-73.43						
		layer 1		layer 2		layer 3		layer 4	
α	in °	0		10		90		70	
z	in mm	-0.25	-0.125	-0.125	0.0	0.0	0.125	0.125	0.25
ε_x	in 10^{-3} mm/mm	1.38	0.53	0.53	-0.31	-0.31	-1.15	-1.15	-1.99
ε_y	in 10^{-3} mm/mm	-30.73	-18.78	-18.78	-6.83	-6.83	5.12	5.12	17.07
γ_{xy}	in 10^{-3} °/°	12.18	3.00	3.00	-6.18	-6.18	-15.36	-15.36	-24.54
$\varepsilon_{\parallel}$	in 10^{-3} mm/mm	1.38	0.53	0.46	-1.56	-6.83	5.12	-0.55	6.95
$\varepsilon_{\perp}$	in 10^{-3} mm/mm	-30.73	-18.78	-18.71	-5.58	-0.31	-1.15	4.52	8.13
$\gamma_{\parallel\perp}$	in 10^{-3} °/°	12.18	3.00	-3.79	-8.04	6.18	15.36	15.79	31.05
$\sigma_{\parallel}$	in MPa	103.1	22.1	13.0	-222.8	-912.3	680.1	-61.5	949.3
$\sigma_{\perp}$	in MPa	-283.8	-174.2	-173.8	-56.2	-20.8	2.7	40.8	94.2
$\tau_{\parallel\perp}$	in MPa	56.0	13.8	-17.4	-37.0	28.4	70.6	72.6	142.8

Only section twist moment m_{xy}:

n_x^0	in N/mm		0						
n_y^0	in N/mm		0						
n_{xy}^0	in N/mm		0						
m_x	in N·mm/mm		0						
m_y	in N·mm/mm		0						
m_{xy}	in N·mm/mm		12						
ε_x^0	in 10^{-3} mm/mm		0.80						
ε_y^0	in 10^{-3} mm/mm		0.26						
γ_{xy}^0	in 10^{-3} °/°		−4.01						
κ_x	in 10^{-3}/mm		−0.51						
κ_y	in 10^{-3}/mm		−44.06						
κ_{xy}	in 10^{-3}/mm		186.93						
		layer 1		layer 2		layer 3		layer 4	
α	in °	0		10		90		70	
z	in mm	−0.25	−0.125	−0.125	0.0	0.0	0.125	0.125	0.25
ε_x	in 10^{-3} mm/mm	0.92	0.86	0.86	0.80	0.80	0.73	0.73	0.67
ε_y	in 10^{-3} mm/mm	11.27	5.77	5.77	0.26	0.26	−5.25	−5.25	−10.76
γ_{xy}	in 10^{-3} °/°	−50.74	−27.38	−27.38	−4.01	−4.01	19.35	19.35	42.72
$\varepsilon_\parallel$	in 10^{-3} mm/mm	0.92	0.86	−3.68	0.09	0.26	−5.25	1.67	4.31
$\varepsilon_\perp$	in 10^{-3} mm/mm	11.27	5.77	10.30	0.96	0.80	0.73	−6.19	−14.40
$\gamma_{\parallel\perp}$	in 10^{-3} °/°	−50.74	−27.38	−24.05	−3.95	4.01	−19.35	−18.67	−40.07
$\sigma_\parallel$	in MPa	152.6	129.7	−463.4	14.9	36.5	−698.5	206.7	537.3
$\sigma_\perp$	in MPa	107.8	56.2	86.7	9.2	8.1	−6.9	−53.5	−123.4
$\tau_{\parallel\perp}$	in MPa	−233.4	−125.9	−110.6	−18.2	18.5	−89.0	−85.9	−184.3

5 Application

Definitions for the layer orientation angle α and the stacking sequence (layer numbering) (as given in Fig. 1) as well as orientation of section forces and section moments (refer to Fig. 3) are commonly used in CLT applications in the way shown in the present document. However, one should be aware that some program systems (e.g. FEM installations) use deviating definitions and one needs to check whether these definitions coincide with each other. If necessary, signs and stacking sequences should be adapted or changed.

Finally, some remarks are added:

- In principle, the elasticity relationships above are the same as for the isotropic plate and they describe the behaviour of the thin laminate.
- In a general lay-up case, there is no plate-parallel symmetry surface which would allow to separate the membrane problem and the bending problem from each other. This would be only possible if the coupling matrix vanished ($[B] = 0$).
- The shear moduli G_{zx}, G_{yz} of most of the composites are significantly smaller than those of isotropic plate material. Therefore, the influence of the transverse (or inter-laminar) shear stresses τ_{zx}, τ_{yz} and of the corresponding strains may only be neglected if the slenderness ratio ℓ/t is larger than a certain limit which depends on the grade of anisotropy. Test calculations of a composite plate with $\ell/t = 20$ and $E_x/G_{zx} = 50$ loaded perpendicular to its surface have revealed an error of 20% for the predicted deflection w^0, if transverse shear was neglected.
- Usually, the elasticity properties are obtained from so-called 'isolated' test specimens (weakest link failure behaviour) whereas an embedded layer is subject to a redundant in-situ behaviour meaning that the embedded layer will not completely lose its stiffness after the first inter-fiber crack.

Acknowledgment

The content of this document has been taken from the HSB (Handbuch Struktur Berechnung) issued by the IASB (Industrie-Ausschuss Struktur-Berechnungsunterlagen). The IASB is thanked for supporting the eLamX project with the present contribution.